9

C-Vector for Identifying Oceanic Secondary Circulations

Secondary circulation, referring to the motion, relative to a basic flow (geostrophic and hydrostatic balanced), occurs often in the ocean such as deep convection and circulations driven by fronts and eddies. It affects the general circulation and the mass, heat, salt, and energy balance. The oceanic secondary circulation is difficult to measure directly, but is easy to be identified by pseudovorticity using the C-vector method from routine temperature and salinity observations.

9.1 C-Vector

The thermal wind relation (1.3) can be rewritten by

$$f\frac{\partial u}{\partial z} = -\frac{\partial b}{\partial y}, \quad f\frac{\partial v}{\partial z} = \frac{\partial b}{\partial x}, \quad b = -g\frac{(\rho - \rho_0)}{\rho_0}, \tag{9.1}$$

where the variable b is usually called the buoyancy. The total flow, $\hat{\mathbf{V}} = (u, v, w)$, is decomposed into geostrophic ($\mathbf{V}$) and ageostrophic ($\mathbf{V}_{\mathrm{ag}}$) velocities,

$$\hat{\mathbf{V}} = \mathbf{V} + \mathbf{V}_{\mathrm{ag}}.$$

If the advection of momentum and buoyancy is dominated by the geostrophic advection (i.e., quasigeostrophic system),

$$\hat{\mathbf{V}} \cdot \nabla\hat{\mathbf{V}} \approx \mathbf{V} \cdot \nabla\mathbf{V}, \quad \hat{\mathbf{V}} \cdot \nabla b = \mathbf{V} \cdot \nabla b, \tag{9.2}$$

then the ageostrophic velocity is determined by Bannon and Chu (1988)

$$-fv_{\mathrm{ag}} = \frac{1}{\rho_0}\frac{\partial X}{\partial z} - \left(\frac{\partial}{\partial t} + \mathbf{V}\cdot\nabla\right)u, \tag{9.3}$$

$$fu_{\mathrm{ag}} = \frac{1}{\rho_0}\frac{\partial Y}{\partial z} - \left(\frac{\partial}{\partial t} + \mathbf{V}\cdot\nabla\right)v, \tag{9.4}$$

$$N^2 w_{\mathrm{ag}} = \frac{\partial B}{\partial z} - \left(\frac{\partial}{\partial t} + \mathbf{V}\cdot\nabla\right)b, \tag{9.5}$$

where (X, Y) and B are the vertical turbulent momentum and buoyancy fluxes (downward positive), and N is the Brunt–Vaisala frequency.

Cross derivatives among (9.3)–(9.5) lead to the definition of pseudovorticity (Xu 1992; Chu 2002),

$$\frac{\partial}{\partial y}(N^2 w_{\mathrm{ag}}) - \frac{\partial}{\partial z}(f^2 v_{\mathrm{ag}}) = 2f^3 C_x, \tag{9.6a}$$

$$\frac{\partial}{\partial z}(f^2 u_{\mathrm{ag}}) - \frac{\partial}{\partial x}(N^2 w_{\mathrm{ag}}) = 2f^3 C_y, \tag{9.6b}$$

$$\frac{\partial}{\partial x}(f^2 v_{\mathrm{ag}}) - \frac{\partial}{\partial y}(f^2 u_{\mathrm{ag}}) = 2f^3 C_z, \tag{9.6c}$$

where

$$C_x = -\frac{1}{f^2}\frac{\partial(u,v)}{\partial(y,z)} + \frac{1}{2f^3}\frac{\partial}{\partial z}\left(f\frac{\partial X}{\partial z} + \frac{\partial B}{\partial y}\right), \tag{9.7a}$$

$$C_y = -\frac{1}{f^2}\frac{\partial(u,v)}{\partial(z,x)} + \frac{1}{2f^3}\frac{\partial}{\partial z}\left(f\frac{\partial Y}{\partial z} - \frac{\partial B}{\partial x}\right), \tag{9.7b}$$

$$C_z = -\frac{1}{f^2}\frac{\partial(u,v)}{\partial(x,y)} - \frac{1}{2f^2}\frac{\partial}{\partial z}\left(\frac{\partial X}{\partial x} + \frac{\partial Y}{\partial y}\right) - \frac{\beta}{2f^3}\frac{\partial Y}{\partial z}, \tag{9.7c}$$

are (nondimensional) components of vector **c**. Thus, the pseudovorticity of the secondary circulation is determined by three forcing factors (a) geostrophic forcing (i.e., distinct water masses across the front), $-f\partial(u,v)/\partial(y,z)$, $-f\partial(u,v)/\partial(z,x)$, and $-f\partial(u,v)/\partial(x,y)$, (b) turbulent momentum flux (X, Y), and (c) buoyancy flux (B). In the upper ocean, the last two factors are mainly caused by the surface wind stress and buoyancy flux. As pointed by Xu (1992), the C-vector is the ageostrophic vortex line (Fig. 9.1) whose horizontal components (C_x, C_y) represent the secondary circulation in vertical cross section.

Observations generally show a well-mixed upper ocean by turbulent motion. The transition between the turbulent mixed layer and the stratified water below is a thin entrainment zone with large gradients of density and

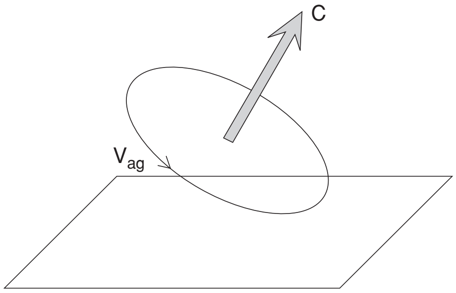

Fig. 9.1. C-vector and the secondary circulation (from Chu 2002, Geophysical Research Letters)

velocity. All turbulent fluxes are usually assumed to vanish below the ocean mixed layer. The mixed layer depth h_1 is defined as the depth above which temperature, salinity, or velocity (geostrophic plus ageostrophic) is vertically uniform to certain critical value. The vertical uniformity leads to the bulk model parameterization (e.g., Price et al. 1986; Chu et al. 1990; Chu and Garwood 1990, 1991) of turbulent fluxes (X, Y, B),

$$(X, Y) = (\tau_x, \tau_y) + \left[(\tau_x, \tau_y) - (X, Y)_{-h}\frac{z}{h_1}\right],$$

$$B = B_0 + (B_0 - B_{-h})\frac{z}{h_1}, \quad \text{for } z > -h_1, \tag{9.8a}$$

$$(X, Y, B) \simeq 0, \quad \text{for } z < -h_1 \tag{9.8b}$$

where (τ_x, τ_y) is the surface wind stress and B_0 is the surface buoyancy flux. $(X, Y)_{-h}$ and B_{-h} are turbulent fluxes at the base of the mixed layer, which are computed from the surface fluxes.

From (9.8a) and (9.8b) we obtain

$$\frac{\partial^2 X}{\partial z^2} = 0, \quad \frac{\partial^2 Y}{\partial z^2} = 0, \tag{9.9}$$

for the whole water column. On computing the horizontal components of the C-vector (C_x, C_y), the turbulent momentum flux can be neglected for the whole water column, and the turbulent buoyancy flux can be neglected for the water column below the surface mixed layer. Note that the nonuniform currents may exist in the upper ocean such as the Ekman layer, where (9.9) does not hold good. However, (9.9) may be used below the Ekman layer.

Since B is a linear function of z in the surface mixed layer [see (9.8a)], the contribution of B to (C_x, C_y) in the surface mixed layer is depth-independent [see (9.8a)]. Since B_{-h} is computed from the surface turbulent fluxes (τ_x, τ_y) and B_0 (bulk models), the atmosphere may control the scale of the horizontal variability of B_{-h} and B_0.

9.2 Secondary Circulations Across Arctic Fronts in the Fram Strait

Fram Strait (Fig. 9.2) is the only deep connection between the Arctic Ocean and the rest of the world ocean through the Greenland Sea, Iceland Sea, and Norwegian Sea (GIN Sea). Water masses in the Fram Strait are imported from the neighboring Atlantic and polar oceans, and are encountered in various stages of modification. The North Atlantic Water is relatively warmer and saline ($T > 2°\text{C}, S > 34.9\,\text{ppt}$). The Polar Water is cooler and fresher ($T < 0°\text{C}, S < 34.7\,\text{ppt}$) (van Aken et al. 1991). Analyzing the 1984 marginal ice zone experiment observations in the Fram Strait, Gascard et al. (1988) found that the West Spitzbergen Current and the East Greenland Current are two main generators for eddies in the Fram Strait.

In the transition, different water masses interface and form frontal zones that not only separate water bodies with different hydrographic characteristics but also the regional biological systems. The different water masses encountered in the GIN Sea and the Fram Strait often form fronts. The Arctic front or frontal zone is oriented more or less meridionally. It separates the warm and salty North Atlantic Water in the Norwegian and West Spitzbergen currents from the cool and fresh Arctic Water (Dietrich 1969). After analyzing hydrographic data along 74°45′N in February 1989 during cruise VA78 of R/V Valdivia, van Aken et al. (1991) identified four Arctic fronts south of the Fram Strait.

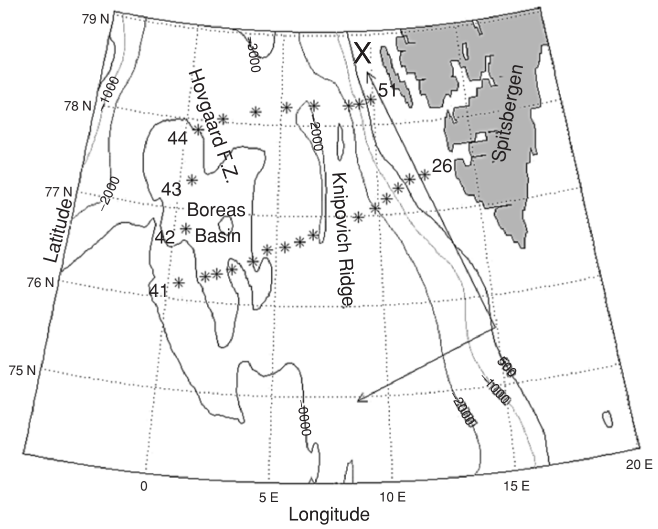

Fig. 9.2. Geography of the East Fram Strait, coordinate system, and CTD stations of R/V Valdivia cruise 54 in the Fram Strait from 16 March to 5 April 1987 (from Chu 2002, Geophysical Research Letters)

The physical–biological effect arises from the significant vertical component of the three-dimensional ageostrophic flow (called the secondary circulation) associated with the fronts, where vertical upward motion may act as a fertilizer of the upper water column. A better knowledge of the secondary circulation is therefore crucial. However, direct measurement of the secondary circulation in the ocean is difficult. The C-vector can be used to diagnose three-dimensional oceanic secondary circulations from observational data.

The atmosphere has most of its energy in scales of several hundreds of kilometers and more, it is reasonable to assume that

$$\frac{\partial}{\partial z}\left(\frac{\partial B}{\partial y}\right) = 0, \quad \frac{\partial}{\partial z}\left(\frac{\partial B}{\partial x}\right) = 0, \tag{9.10}$$

across the Arctic front, and therefore the horizontal C-vector components are computed from the geostrophic forcing only. The geostrophic forcing has been recognized as the major factor to cause the atmospheric frontal secondary circulation (Hoskins et al. 1978; Xu 1992). It may also be important for oceanic frontal secondary circulation.

9.3 Hydrographic Data Collection

CTD data, collected during a large-scale hydrographic survey on RV/VALDIVIA cruise-54 of the eastern Greenland Sea and the Fram Strait from 16 March to 5 April 1987 (Quadfasel and Ungewiß 1988), are used to illustrate the advantage of using the C-vector method in analyzing oceanic secondary circulation. The major task of this cruise was to map the vertical distribution of temperature, salinity, and dissolved oxygen in the Greenland Sea as a measure of the large-scale circulation and transport. A secondary objective was to search active convection events. Along seven sections a total of 73 CTD profiles were taken (Fig. 9.2). Four of these sections crossed the Arctic Front that separates the Greenland Sea gyres from the warm and saline northward flowing Norwegian Atlantic Current and the West Spitzbergen Current. The sections were designed to form three closed boxes to allow calculation of transport budgets. An usual station spacing was 56 km except along the Fram Strait section at $78°25'$N and across the Hovgaard Fracture Zone, where the spacing was decreased to less than 28 km. All CTD profiles were run to the depth of within 5 m of the bottom.

9.4 Potential Density

The potential density excess referred to 500 db computed from the CTD data shows the existence of multifrontal zones in the Fram Strait. For example, three Arctic fronts are identified from the north cross section (Stations 44–51) (Fig. 9.3) (a) eastern front occurring near the west coast of Spitzbergen

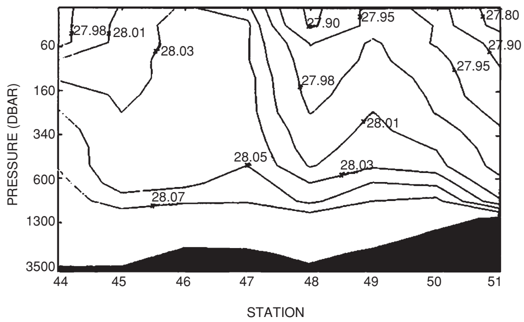

Fig. 9.3. Potential density excess referred to 500 db along the north cross section in the Fram Strait (from Stations 44–51) (from Chu 2002, Geophysical Research Letters)

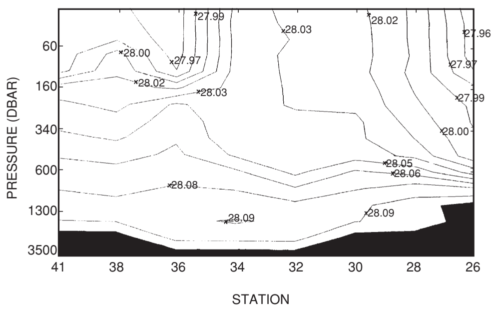

Fig. 9.4. Potential density excess referred to 500 db along the south cross section in the Fram Strait (from Stations 26–41) (from Chu 2002, Geophysical Research Letters)

(Stations 49–51), (b) shallow western front (above 160 m depth) occurring near 0° longitude (Stations 44–46) in the Hovgaard Fracture Zone, and (c) a deep midfront (Stations 47–48) in the north Knipovich Ridge. Within the south cross section in the Fram Strait (Stations 26–41, Fig. 9.4), only two fronts can be identified with a strong and shallow front in the Boreas Basin (Stations 34.36) and a weak deep front near the west coast of Spitzbergen (Stations 26–30).

Usually, upward (downward) bending of isopycnal is used to identify upward (downward) motion. For example, in Fig. 9.3 the isopycnal bend upward near Stations 46–47, 49, and downward near Stations 45 (to 250 m depth), 48 (surface to 1,000 m depth), and 51. Since such identification is very qualitative, it is hard to sketch the secondary circulation pattern and strength. Is it possible to get quantitative information using the same density data? The answer is "yes" because the secondary circulation can be represented by the horizontal component of the C-vector (i.e., horizontal pseudovorticity).

9.5 Horizontal Pseudovorticity

The geostrophic current (u, v) is computed from density, and then the horizontal components of the C-vector are computed from (u, v). Figure 9.5 shows the x-component of the nondimensional pseudovorticity (C_x/f^2) along the north cross section (Stations 44–51). Looking toward north the positive (negative) values of C_x/f^2 imply a clockwise (anticlockwise) circulation. Two clockwise and two anticlockwise secondary circulations are identified. Among them, the clockwise secondary circulations are deeper than the anticlockwise secondary circulations (depth less than 60 m). Note that in this study, the geostrophic current is computed as 2,500 db which is to be assumed as the level of no motion. This may affect the C-vector computation, especially in large horizontally sheared barotropic current such as in the Fram Strait (Fahrbach et al. 2001). However, Fig. 9.5 keeps almost the same geostrophic current as 2,000 db which is chosen as the reference level.

The most striking feature is the existence of a shallow (surface to 60 m), strong anticlockwise secondary circulation with a minimum value of C_x/f^2 around −9.01, located near the Knipovich Ridge (Stations 46–48). We may call it the Knipovich cell. The upward and downward branches of this cell are connected to two clockwise secondary cells from the east (upward branch) and west (downward branch). Below the Knipovich cell, between 340 and 1,000 m depth, there is a very weak clockwise vorticity (a maximum value of C_x/f^2 around 0.01).

East of the Knipovich cell, a deep (surface to 1,000 m), clockwise secondary circulation with a maximum pseudovorticity of 1.95 is identified near the West

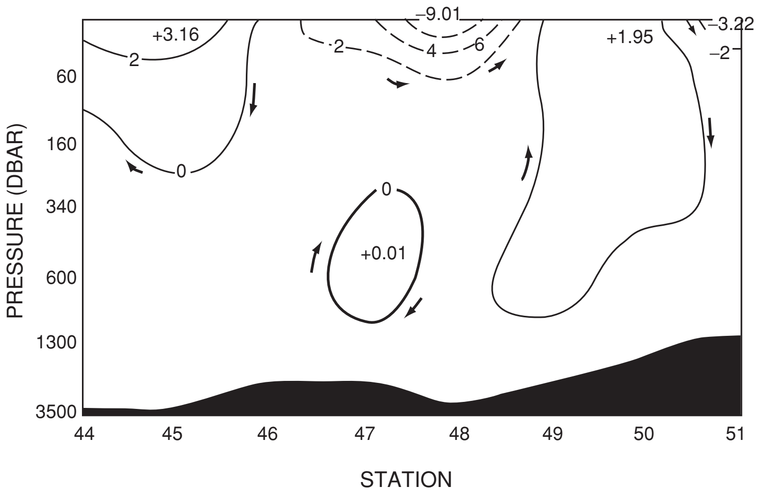

Fig. 9.5. Nondimensional horizontal pseudovorticity, C_x, along the north cross section in the Fram Strait (from Chu 2002, Geophysical Research Letters)

Spitzbergen slope (Stations 48–50). We may call it the West Spitzbergen cell. Its downward branch follows the slope. Its upward branch connects to the Knipovich cell. West of the Knipovich cell, a relatively shallow (to 250 m depth) clockwise secondary circulation with a maximum pseudovorticity of 3.16 is identified in the Hovgaard Fracture Zone (Stations 44–46). The downward branch connects to the Knipovich cell (Stations 46–48). The upward branch is located at Stations 44–45. We may call it the Hovgaard cell. The horizontal pseudovorticity (C_x/f^2) represents the secondary circulation around the x-axis. The larger the C_x/f^2, the secondary circulation is stronger. Strong upwelling is identified between the Knipovich Ridge and the West Spitzbergen slope.

9.6 Two Scalar Functions

For large-scale motion, the horizontal variability of $B_{\text{-}h}$ and B_0 cannot be assumed as zero, and (9.10) is not valid. However, (9.9) can be considered as valid because it does not depend on the horizontal scale. The C-vector for the large-scale motion can be written by

$$C_x = -\frac{1}{f^2}\frac{\partial(u,v)}{\partial(y,z)} + \frac{1}{2f^3}\frac{\partial}{\partial z}\left(\frac{\partial B}{\partial y}\right), \tag{9.11a}$$

$$C_y = -\frac{1}{f^2}\frac{\partial(u,v)}{\partial(z,x)} - \frac{1}{2f^3}\frac{\partial}{\partial z}\left(\frac{\partial B}{\partial x}\right), \tag{9.11b}$$

$$C_z = -\frac{1}{f^2}\frac{\partial(u,v)}{\partial(x,y)} - \frac{1}{2f^2}\frac{\partial}{\partial z}\left(\frac{\partial X}{\partial x} + \frac{\partial Y}{\partial y}\right) - \frac{\beta}{2f^3}\frac{\partial Y}{\partial z} \tag{9.11c}$$

where the thermohaline circulation can be represented by the horizontal components (C_x, C_y) and the wind-driven circulation can be represented by the vertical component C_z.

Defining the two scalar functions used by Chu et al. (2003a, b),

$$u_{\text{ag}} = -\frac{\partial\psi}{\partial y} + \frac{\partial^2\phi}{\partial z\partial x}, \quad v_{\text{ag}} = \frac{\partial\psi}{\partial x} + \frac{\partial^2\phi}{\partial z\partial y}, \quad w_{\text{ag}} = -\nabla_2^2\phi, \tag{9.12}$$

the three-dimensional scalar functions (ψ, ϕ) may be called generalized stream function and velocity potential. Substituting (9.12) into (9.6) yields

$$\frac{1}{f^2}\frac{\partial}{\partial y}\left(N^2\nabla_2^2\phi + f^2\frac{\partial^2\phi}{\partial z^2}\right) - \frac{\partial^2\psi}{\partial x\partial z} = -2fC_x, \tag{9.13a}$$

$$\frac{1}{f^2}\frac{\partial}{\partial x}\left(N^2\nabla_2^2\phi + f^2\frac{\partial^2\phi}{\partial z^2}\right) + \frac{\partial^2\psi}{\partial y\partial z} = 2fC_y, \tag{9.13b}$$

$$\nabla_2^2\psi + \frac{2\beta}{f}\frac{\partial\psi}{\partial y} - \frac{2\beta}{f}\frac{\partial^2\phi}{\partial x\partial z} = 2fC_z. \tag{9.14}$$

Cross differentiation of (9.13a) and (9.13b) yields

$$\frac{\partial}{\partial x}\left[\frac{1}{f^2}\frac{\partial}{\partial x}\left(N^2\nabla_2^2\phi + f^2\frac{\partial^2\phi}{\partial z^2}\right)\right] + \frac{\partial}{\partial y}\left[\frac{1}{f^2}\frac{\partial}{\partial y}\left(N^2\nabla_2^2\phi + f^2\frac{\partial^2\phi}{\partial z^2}\right)\right]$$

$$= 2\left[\frac{\partial}{\partial x}(fC_y) - \frac{\partial}{\partial y}(fC_x)\right]. \tag{9.15}$$

Here, (9.14) and (9.15) are the two diagnostic equations for determining (ψ, ϕ) from hydrographic data. Equation (9.15) shows that the generalized velocity potential (ϕ) is solely forced by the horizontal components of the C-vector (C_x, C_y). However, (9.14) shows that the generalized stream function (ψ) is affected by ϕ, only if the β-effect is considered.

9.7 Three Types of Forcing Terms for Ageostrophic Circulation

Substituting (9.11) into (9.14) and (9.15) yield

$$\nabla_2^2\psi + \frac{2\beta}{f}\frac{\partial\psi}{\partial y} - \frac{2\beta}{f}\frac{\partial^2\phi}{\partial x\partial z} = S_{\text{geo}}^{(\psi)} + S_{\text{w}}, \tag{9.16}$$

$$\frac{\partial}{\partial x}\left[\frac{1}{f^2}\frac{\partial}{\partial x}\left(N^2\nabla_2^2\phi + f^2\frac{\partial^2\phi}{\partial z^2}\right)\right] + \frac{\partial}{\partial y}\left[\frac{1}{f^2}\frac{\partial}{\partial y}\left(N^2\nabla_2^2\phi + f^2\frac{\partial^2\phi}{\partial z^2}\right)\right]$$

$$= S_{\text{geo}}^{(\phi)} + S_{\text{B}}, \tag{9.17}$$

where

$$S_{\text{geo}}^{(\psi)} \equiv -\frac{2}{f}\frac{\partial(u,v)}{\partial(x,y)}, \quad S_{\text{geo}}^{(\phi)} \equiv -2\left\{\frac{\partial}{\partial x}\left[\frac{1}{f}\frac{\partial(u,v)}{\partial(z,x)}\right] - \frac{\partial}{\partial y}\left[\frac{1}{f}\frac{\partial(u,v)}{\partial(y,z)}\right]\right\}, \tag{9.18}$$

are the geostrophic forcing terms;

$$S_{\text{w}} \equiv -\frac{1}{f}\frac{\partial}{\partial z}\left(\frac{\partial X}{\partial x} + \frac{\partial Y}{\partial y}\right) - \frac{\beta}{f^2}\frac{\partial Y}{\partial z}, \tag{9.19}$$

is the wind forcing term; and

$$S_{\text{B}} \equiv -\left[\frac{\partial}{\partial x}\left(\frac{1}{f^2}\frac{\partial^2 B}{\partial z\partial x}\right) - \frac{\partial}{\partial y}\left(\frac{1}{f^2}\frac{\partial^2 B}{\partial z\partial y}\right)\right], \tag{9.20}$$

is the buoyancy forcing term. Without the β-effect ($\beta = 0$), the two functions (ψ, ϕ) can be independently solved from

$$\nabla_2^2\psi = S_{\text{geo}}^{(\psi)} + \bar{S}_{\text{w}}, \tag{9.21}$$

$$\nabla_2^2\left(N^2\nabla_2^2\phi + f^2\frac{\partial^2\phi}{\partial z^2}\right) = \bar{S}_{\text{geo}}^{(\phi)} + \bar{S}_{\text{B}}, \tag{9.22}$$

where

$$\bar{S}_{\text{geo}}^{(\phi)} \equiv 2f\left[\frac{\partial}{\partial y}\frac{\partial(u,v)}{\partial(y,z)} - \frac{\partial}{\partial x}\frac{\partial(u,v)}{\partial(z,x)}\right], \quad \bar{S}_{\text{B}} \equiv -\nabla_2^2\left[\frac{(B_0 - B_{-h})}{h_1}\right],$$

$$\bar{S}_{\text{w}} \equiv -\frac{1}{f}\frac{\partial}{\partial z}\left(\frac{\partial X}{\partial x} + \frac{\partial Y}{\partial y}\right). \tag{9.23}$$

Thus the two scalar functions (ψ, ϕ) can be obtained independently.

Questions and Exercises

(1) What features can you get between $\nabla \times \mathbf{C}$ and the ageostrophic velocity $\mathbf{V}_{\text{ag}}$? Here, $\mathbf{V}_{\text{ag}} = (u_{\text{ag}}, v_{\text{ag}}, w_{\text{ag}}), \mathbf{C} = (C_x, C_y, C_z)$,

$$\frac{\partial}{\partial y}(N^2 w_{\text{ag}}) - \frac{\partial}{\partial z}(f^2 v_{\text{ag}}) = 2f^3 C_x, \tag{E9.1}$$

$$\frac{\partial}{\partial z}(f^2 u_{\text{ag}}) - \frac{\partial}{\partial x}(N^2 w_{\text{ag}}) = 2f^3 C_y, \tag{E9.2}$$

$$\frac{\partial}{\partial x}(f^2 v_{\text{ag}}) - \frac{\partial}{\partial y}(f^2 u_{\text{ag}}) = 2f^3 C_z, \tag{E9.3}$$

(2) What is the divergence of $\mathbf{C}$?

(3) Discuss the feasibility of using the linear representation of the turbulent momentum and buoyancy fluxes in the mixed layer

$$(X, Y) = (\tau_x, \tau_y) + \left[(\tau_x, \tau_y) - (X, Y)_{-h}\frac{z}{h_1}\right], \tag{E9.4}$$

$$B = B_0 + (B_0 - B_{-h})\frac{z}{h_1}, \quad \text{for } z > -h_1, \tag{E9.5}$$

$$(X, Y) \simeq 0, \quad \text{for } z < -h_1, \tag{E9.6}$$

where h_1 is the mixed layer depth, (τ_x, τ_y) is the surface wind stress, and B_0 is the surface buoyancy flux. $(X, Y)_{-h}$ and B_{-h} are turbulent fluxes at the base of mixed layer, which are computed from the surface fluxes.

(4) Discuss the difference of the turbulent momentum flux represented by (E9.4) and the Ekman flow model.

(5) Why the conditions

$$\frac{\partial}{\partial z}\left(\frac{\partial B}{\partial y}\right) = 0, \quad \frac{\partial}{\partial z}\left(\frac{\partial B}{\partial x}\right) = 0, \tag{E9.7}$$

are realistic across the Arctic Front?

(6) Discuss the characteristics for the potential density field shown in Figs. 9.3 and 9.4? Can you identify Polar Front on these figures?
(7) What are the major characteristics of the secondary circulation across the Fram Strait as shown in Fig. 9.5?
(8) Discuss the physical significance of (ψ, ϕ) equations for the ageostrophic flow,

$$\nabla_2^2 \psi + \frac{2\beta}{f}\frac{\partial \psi}{\partial y} - \frac{2\beta}{f}\frac{\partial^2 \phi}{\partial x \partial z} = S_{\text{geo}}^{(\psi)} + S_{\text{w}}, \tag{E9.8}$$

$$\frac{\partial}{\partial x}\left[\frac{1}{f^2}\frac{\partial}{\partial x}\left(N^2\nabla_2^2\phi + f^2\frac{\partial^2\phi}{\partial z^2}\right)\right] + \frac{\partial}{\partial y}\left[\frac{1}{f^2}\frac{\partial}{\partial y}\left(N^2\nabla_2^2\phi + f^2\frac{\partial^2\phi}{\partial z^2}\right)\right]$$
$$= S_{\text{geo}}^{(\phi)} + S_{\text{B}}. \tag{E9.9}$$

(9) Discuss dynamically the difference between the two scalar functions (ψ, ϕ). Why does the β-effect connect the ϕ-function to the ψ-function?
(10) Since the scalar ϕ is determined by buoyancy and geostrophic forcing, can you use ϕ to represent the thermohaline circulation? Why?
(11) The ψ-function is basically forced by the winds and geostrophic flow. Why equation (E9.8) is so different from the stream function in the wind-driven-circulation models such as the Stommel model?